

Rational Synthesis of Crystalline Covalent Triazine Framework with Methylthio Pendant Arms for Efficient Mercury (II) Adsorption

LOU Yi-xiao^{1,2}, ZHOU Lu-lu³, YANG Na¹, ZHU Xiang^{1*}

(1. State Key Laboratory for Oxo Synthesis and Selective Oxidation, Lanzhou Institute of Chemical Physics, Chinese Academy of Sciences, Lanzhou 730000, China; 2. University of Chinese Academy of Sciences, Beijing 100049, China; 3. School of Resources and Environment Engineering, East China University of Science and Technology, Shanghai 200237, China)

Abstract: The interest in curtailing environmental pollution issues through physical separation processes has inspired an extensive search for novel nanoporous materials with exceptional adsorption capabilities. Covalent triazine frameworks (CTFs), emerged as a class of crystalline covalent organic frameworks (COFs), have been widely examined for various separation applications, owing to their large porosity, high stability, and rich nitrogen (N) doping. The development of CTFs for efficient adsorption of mercury (II) (Hg^{2+}) is of great importance for the field, whereas it is rarely attempted, on account of limited synthetic strategies and unknown structural-property relations of conventional CTFs derived from ionothermal approaches. Herein, we report rational synthesis of a crystalline CTF with methylthio pendant arms for efficient removal of Hg^{2+} with an exceptional capacity of $751 \text{ mg}\cdot\text{g}^{-1}$, ranking at the top among previously-reported adsorbents. This work may open up new possibility in the synthesis of COFs for various separations.

Key words: CTFs; methylthio pendant arms; mercury adsorption; structural-property relationship

CLC number: O643.12

Document code: A

DOI: 10.16084/j.issn1001-3555.2024.04.002

Recently, environmental pollution issues, for example, the emission of carbon dioxide and the removal of heavy metals from power plants, industrial facilities and human activities, have attracted tremendous attention^[1-2]. Heavy metals, such as mercury (Hg^{2+}), with poor degradability and high solubility in solutions, are extremely harmful for human health, since they could be cycled through the food chain and enriched to the human body, damaging central systems^[3-7]. In this regard, numerous strategies have been developed for efficient removal of Hg^{2+} . Among various techniques, physical adsorption process represents one of the most promising methods, due to its low cost, simplicity and high efficiency^[8-12]. And significant research efforts have been devoted into the search and development of efficient nanoporous adsorbents. A wide variety of advanced porous materials, like, activated nanoporous carbon^[13], mesoporous silica^[14], zeolites^[15], porous organic polymer^[16], metal organic frameworks^[17] and covalent organic frameworks^[18] have been prepared and attempted for this application.

Covalent triazine frameworks (CTFs) emerged as a novel class of COFs, are typically constructed through trimerization of aromatic nitriles. They have been widely explored in the field of adsorption and separation because of their permanent porosity, high physicochemical stability, and rich nitrogen-containing sites^[19-20]. For instance, Qin and co-workers have developed a triazine-based porous organic polymer with a maximum mercury uptake of $658.9 \text{ mg}\cdot\text{g}^{-1}$ ^[21]. Voort's group^[22]

recently developed a CTF encapsulated with $\gamma\text{-Fe}_2\text{O}_3$ nanoparticles, where the Hg^{2+} adsorption capacity was achieved to be $165.8 \text{ mg}\cdot\text{g}^{-1}$. Furthermore, it has been well documented that sulfur-based groups are privileged receptors towards Hg^{2+} . As such, these active moieties, such as methylthio units have been extensively introduced into the framework of porous adsorbents, so as to boost the adsorption performance^[23-26]. Nevertheless, conventional preparation methods for the construction of CTFs through high-temperature-involved ZnCl_2 -promoted ionothermal processes significantly restrict the installation of functional methylthio groups within pore walls, on account of partial carbonization of these CTF frameworks under such high synthetic temperatures^[27-28]. Accordingly, it is rather difficult to obtain an accurate structure-property relationship for the removal of Hg^{2+} using CTF-based adsorbents.

With these considerations in mind, we report rational synthesis of a crystalline CTF with methylthio pendant arms for efficient Hg^{2+} adsorption. The key of our preparation lies in a low-temperature-processed condensation reaction between methylthio-functionalized aromatic aldehydes and amidine moieties for the preparation of triazine-linked crystalline frameworks, which avoids the partial carbonization of task-specific methylthio (MT) groups and gives rise to deeper understanding of effect of methylthio groups on the adsorption of Hg^{2+} within CTF. As a result, the resulting adsorbent (MT-CTF) exhibits an exceptional uptake capacity towards Hg^{2+} , as high as $751 \text{ mg}\cdot\text{g}^{-1}$, accompanied with high selectivity over a

Received date: 2024-03-26; **Revised date:** 2024-04-09.

Foundation: The National Natural Science Foundation of China (22078349, 22005319 and 52170109); Self-deployment Program from Lanzhou Institute of Chemical Physics (E30159SQ).

Biography: Lou Yi-xiao(1998-), female, master degree candidate, mainly engaged in research of the preparation of novel porous organic polymers and applications in pollutant treatment and CO_2 utilization. E-mail: yixiaolou1998@163.com.

* Corresponding authors. E-mail: xiang@licp.cas.cn.

wide range of metal ions. We expect that our findings will open up new possibility in the synthesis of CTFs for promising separation applications.

1 Experimental section

1.1 Chemicals

Terephthalaldehyde, *N,N*-dimethylformamide (DMF), potassium carbonate (K_2CO_3), tetrahydrofuran (THF), dichloromethane, methanol, ethanol and a series of ionic standard solutions were purchased from National Medicines Corporation Ltd. of China. 2,5-dibromoterephthalaldehyde, benzene-1,4-dicarbonitrile, and a series of nitrates were obtained from Aldrich Chemical Co., Inc.

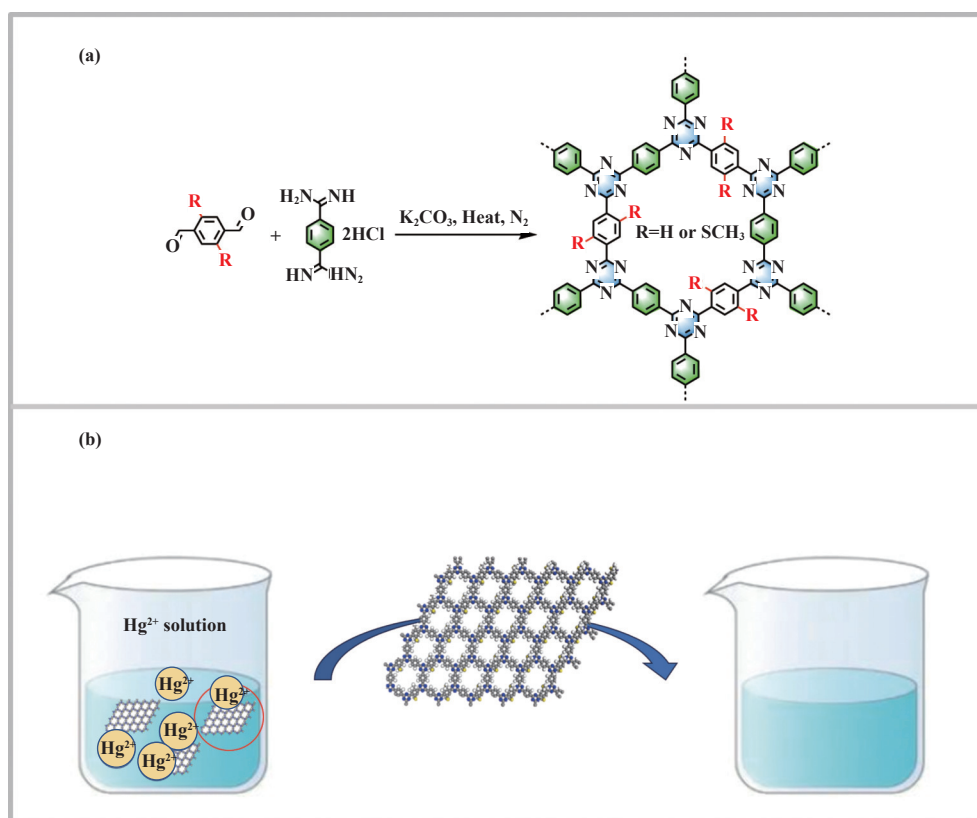
1.2 Materials preparation

2,5-bis(methylthio)terephthalaldehyde was prepared following the literature [29]. The desired compound was achieved with a yield of 87%. 1H NMR (400 MHz, $CDCl_3$) δ : 10.42 (s, 2H), 7.80 (s, 2H), 2.58 (s, 6H); ^{13}C NMR (101 MHz, $CDCl_3$) δ :

16.5, 130.1, 136.3, 139.8, 190.7.

The terephthalamidine dihydrochloride was synthesized according to the reported procedure [28]. The desired compound was recrystallized from the H_2O -EtOH mixture with a yield of 85%. 1H NMR (400 MHz, $DMSO-d_6$) δ : 8.07 (s, 2H), 7.92 (s, 4H), 7.49 (s, 2H). ^{13}C NMR (101 MHz, D_2O) δ : 169.80, 137.82, 133.83.

As shown in Scheme 1, the synthesis of MT-CTF adsorbent was shown as the following: 22.6 mg (0.1 mmol) 2,5-bis(methylthio)terephthalaldehyde, 48 mg (0.3 mmol) benzene-1,4-dicarboximidamide dihydrochloride, and 28 mg (0.2 mmol) K_2CO_3 were added into the flask (50 mL), then the mixture was degassed, DMF (5 mL) was added subsequently, then the reaction took place under N_2 at 80 °C for 24 h, at 120 °C for 48 h, and at 150 °C for 72 h, respectively. After that, the precipitate was washed with various solvents to afford MT-CTF. The yellow product was then dried under vacuum at 60 °C for 12 h. Controlled sample CTF-1 was synthesized according to the literature [30].



Scheme 1 Synthetic scheme and structures of CTFs

1.3 Catalyst characterization

The Bruker model VERTEX 70 infrared spectrometer was used to characterize the Fourier transform infrared spectroscopy (FT-IR) of CTFs. Nuclear Magnetic Resonance (1H NMR and ^{13}C NMR) spectra were performed on a Bruker AV400 (400 MHz for proton, 101 MHz for carbon) spectrometer with tetramethyl silane as the internal reference. The Brunauer-Emmett-Teller (BET) surface area of MT-CTF and CTF-1 were recorded using a Micrometrics 3flex surface area analyzer. The CO_2 adsorption of the MT-CTF and CTF-1 were tested at 25 °C simultaneously. The Bruker 500 MHz/

AVANCE III spectrometer was used to characterize the ^{13}C cross polarization magic angle spinning nuclear magnetic resonance (CP/MAS ^{13}C -NMR) spectroscopy of the CTFs. Scanning electron microscopy (SEM) measurements were conducted with a Hitachi SU 8000 instrument. Thermogravimetric analysis (TGA) was performed under the nitrogen flow with a heating rate of $10\text{ }^\circ\text{C}\cdot\text{min}^{-1}$ using a Mettler Toledo TGA/DSC1 Simultaneous Thermal Analyzer (up to 800 °C). Bruker RFS 100/S spectrometer and PHI 5000 VersaProbe were used to determine the X-ray photoelectron spectroscopy (XPS) spectra of MT-CTF and CTF-1. The concentrations of

Hg²⁺ were analyzed by the Inductively Coupled Plasma-Mass Spectrometry (ICP-MS) and Inductively Coupled Plasma-Optical emission spectroscopy (ICP-OES) (Agilent 725-ES).

1.4 Hg²⁺ batch adsorption experiments

The initial Hg²⁺ stock solution (800 mg·L⁻¹) was prepared by dissolving Hg(NO₃)₂ (0.3246 g) into distilled water (250 mL). The initial Hg²⁺ solution underwent dilution to obtain different concentrations of Hg²⁺ solutions. HNO₃ and NaOH solutions were used to adjust the pH value of the solution. The concentrations of Hg²⁺ were determined by ICP-OES (mg·L⁻¹ level) and ICP-MS (μg·L⁻¹ level). The adsorption experiments were conducted under ambient conditions.

1.5 Hg²⁺ adsorption isotherm analysis

To obtain Hg²⁺ adsorption isotherms, 5 mg of adsorbent (MT-CTF and CTF-1) was added to 10 mL of Hg²⁺ aqueous solutions (ranging from 25 to 800 mg·L⁻¹). The solution was sonicated and then stirred for 12 h. After the adsorption, the remaining Hg²⁺ in the filtrate was determined by ICP-OES. Subsequently, the adsorption capacity (q_e) was determined based on the following equation (1), where C_0 is the initial concentration, C_e is the equilibrium concentrations, V is the volume of the solution treated (mL), m signifies the amount of adsorbent utilized (mg). Unless otherwise specified, the C_0 , C_e , V and m in the following paragraphs is consistent with the above.

$$q_e = \frac{(C_0 - C_e) \times V}{m} \quad (1)$$

1.6 Hg²⁺ adsorption kinetics

A flask containing 5 mg·L⁻¹ Hg²⁺ solution (200 mL), then MT-CTF (20 mg) was added. This mixture was sonicated to disperse, and stirred continuously for 12 h. After the uptake, the residual Hg²⁺ concentration was determined by ICP-MS.

1.7 Effect of pH on adsorption

5 mg of MT-CTF was added into 10 mL Hg²⁺ solution (10 mg·L⁻¹). The pH of the solution was adjusted with 0.1 mol·L⁻¹ HNO₃ or NaOH, and then stirred overnight.

1.8 Selectivity tests

20 mg of MT-CTF was added to a solution of Hg(NO₃)₂, Be(NO₃)₂, Mg(NO₃)₂, Al(NO₃)₃, Mn(NO₃)₂, Co(NO₃)₂, Ni(NO₃)₂, Cu(NO₃)₂, Zn(NO₃)₂, Cd(NO₃)₂, Ba(NO₃)₂ (each 5 mg·L⁻¹, 200 mL). The removal efficiency (η) was calculated using the following equation (2):

$$\eta = \frac{(C_0 - C_e) \times V}{C_0} \times 100\% \quad (2)$$

1.9 Recyclability test

The adsorbed material (Hg@MT-CTF) was stirred in a concentrated HCl solution (12 mol·L⁻¹) for 3 h. The solid was then collected by centrifugation, and washed with diluted HCl solution repeatedly. After that, the material was washed thoroughly until the filtrate solution reached a neutral pH value and collected by filtration, and then the material was dried under vacuum to afford MT-CTF.

2 Results and discussion

2.1 Structural characterization

Powder X-ray diffraction (PXRD) patterns were recorded to validate the crystalline structure. As shown in Fig. 1(a), as expected, due to the reflection from the (010) and (020) crystal facets of MT-CTF, distinguishable peaks at 7.6° and 13.8° were

acquired, respectively. Pawley refinements give rise to optimized parameters ($a = b = 1.488$ nm, and $c = 0.366$ nm), matching well with the eclipsed AA-stacking model ($R_{wp} = 8.14\%$ and $R_p = 6.03\%$). The powder X-ray diffraction (PXRD) of CTF-1 displays diffraction peaks at 7.3°, 12.7°, 14.6° and 25.8°, assigned to the (100), (110), (200) and (001) crystal facets, respectively (Fig. 1(c)). The nitrogen adsorption isotherms were collected at -196 °C, where the BET value of MT-CTF and CTF-1 was calculated to be 483 and 627 m²·g⁻¹ (Fig. 1(e) and Fig. 1(g)). The CO₂ binding affinity of MT-CTF was also examined by measuring the CO₂ uptake (Fig. 1(f) and Fig. 1(h)), which was measured to be 1.66 mmol·g⁻¹ at 25 °C and larger than that of CTF-1 (0.68 mmol·g⁻¹). This may be attributed to the presence of abundant methylthio sites within MT-CTF [31-32].

To verify the as-obtained CTFs, the chemical constitution of MT-CTF and CTF-1 was further analyzed using FT-IR and CP/MAS ¹³C-NMR spectroscopy. As shown in Fig. 2(c), two strong absorption bands at 1515 and 1354 cm⁻¹ represent the aromatic C—N stretching and “breathing” modes in the triazine unit of MT-CTF, respectively [33-34], where an absorbance band at 2920 cm⁻¹ successfully indicates the absorption of the methylthio groups [35]. Their chemical structures were further confirmed by solid-state ¹³C NMR spectra (Fig. 2(a) and Fig. 2(b)). The signal of *sp*² carbons from the triazine ring was revealed by the peak around (δ : ~168) [28]. The signal at $\delta=15$ was assigned to C—S of methylthio groups [36], suggesting the successful installation of methylthio groups within the architecture of MT-CTF. Moreover, the EDS images of MT-CTF further confirm the existence of N/S-containing sites (Fig. 3(a)). Additionally, exceptional thermal stability without significant weight loss up to 300 °C was achieved based on thermogravimetric analysis (TGA) under the N₂ atmosphere (Fig. 3(b)).

2.2 Hg²⁺ adsorption performance

To access separation efficiency, MT-CTF was added into aqueous Hg(NO₃)₂ solutions with Hg²⁺ concentrations, ranged from 25 to 800 mg·L⁻¹. After reaching equilibrium, the uptake capacities were examined by ICP experiments. The equilibrium adsorption data closely aligned with both the Langmuir and Freundlich isotherm models, with excellent correlation coefficients ($R^2 > 0.98$) (Fig. 4(a)). In addition, we further studied the adsorption kinetics of the removal of Hg²⁺ (Fig. 4(b)). Within the initial 30 minute, approximately 80% of the Hg²⁺ can be captured. After 12 h, the concentration of residual Hg²⁺ in the aqueous solution dropped to less than 1 μg·L⁻¹, meeting the U.S. Environmental Protection Agency's standard (< 2 μg·L⁻¹). The adsorption kinetic data was fitted with the pseudo-second-order kinetic model from pseudo-second-order kinetic equation (3):

$$\frac{t}{q_t} = \frac{1}{k_2 q_e^2} + \frac{t}{q_e} \quad (3)$$

where t is the specific time (min), q_t is the Hg²⁺ uptake capacities at time t , q_e is the Hg²⁺ uptake capacities at time equilibrium (mg·g⁻¹), k_2 is the adsorption rate constant (g·mg⁻¹·min⁻¹).

As shown in Fig. 4(c), the adsorption rate constant k_2 is 0.0203 g·mg⁻¹·min⁻¹, which indicated rapid removal of Hg²⁺ from the solution. The suitability of pseudo-second-order kinetics has been demonstrated according to previous reports.

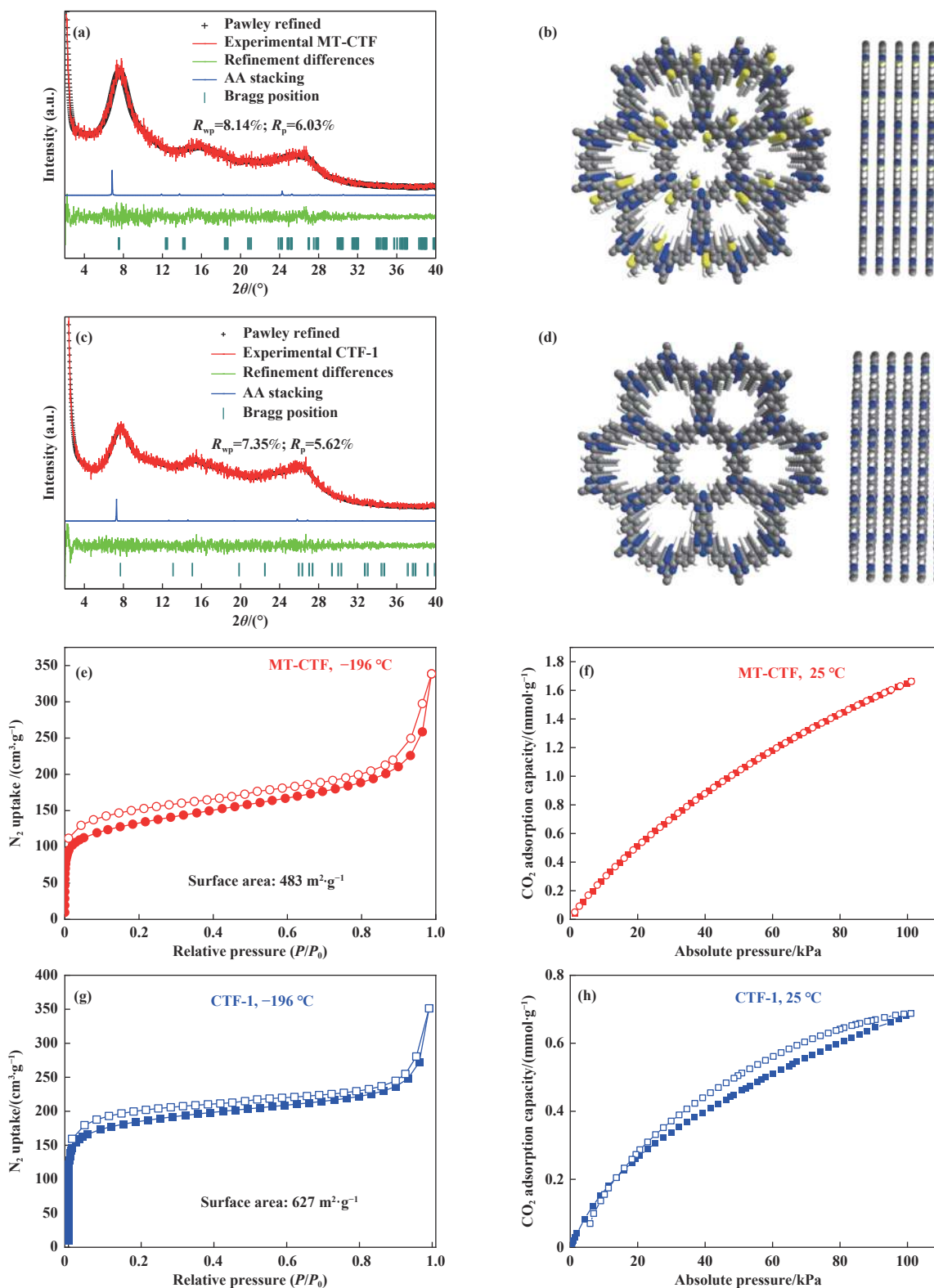


Fig.1 Experimental PXRD patterns and simulated results of MT-CTF (a) and CTF-1 (c), respectively; (b) and (d) Top and side views of the space-filling models (Color code: H, white; C, grey; N, blue; S, yellow); Nitrogen adsorption isotherms of MT-CTF (e) and CTF-1 (g) collected at $-196\text{ }^\circ\text{C}$, and CO_2 adsorption-desorption curves of MT-CTF (f) and CTF-1 (h) at $25\text{ }^\circ\text{C}$

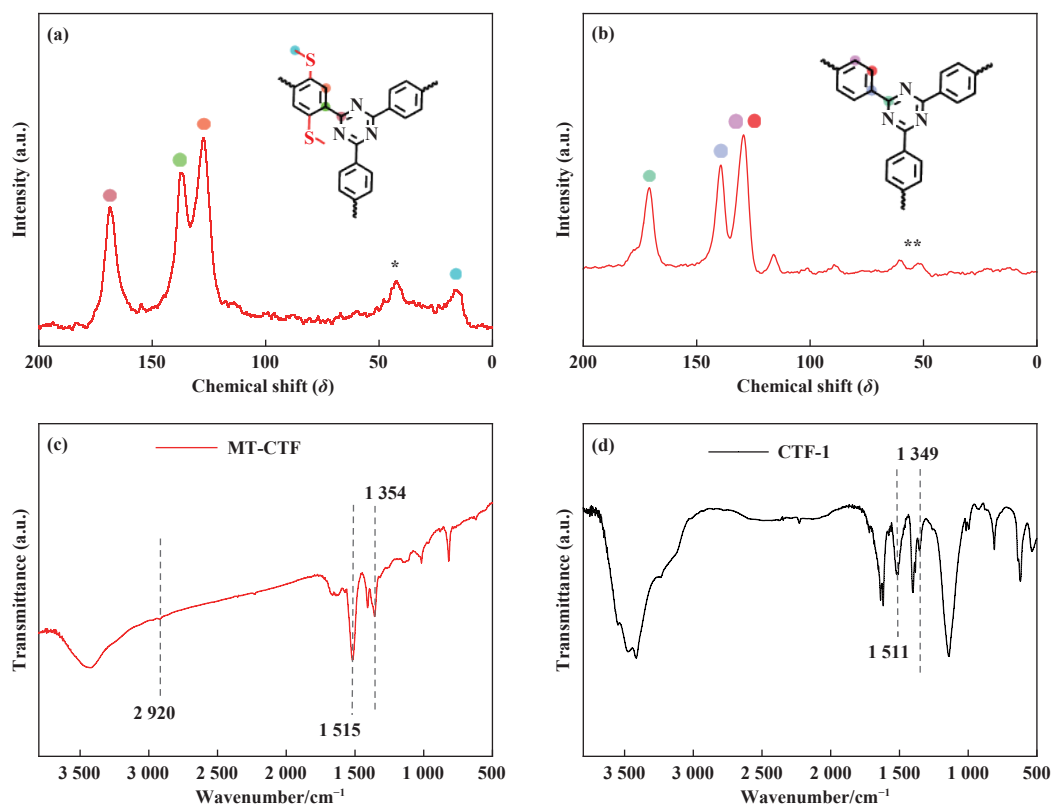


Fig.2 ^{13}C NMR spectra of (a) MT-CTF and (b) CTF-1; Fourier transform infrared (FT-IR) spectra of (c) MT-CTF and (d) CTF-1

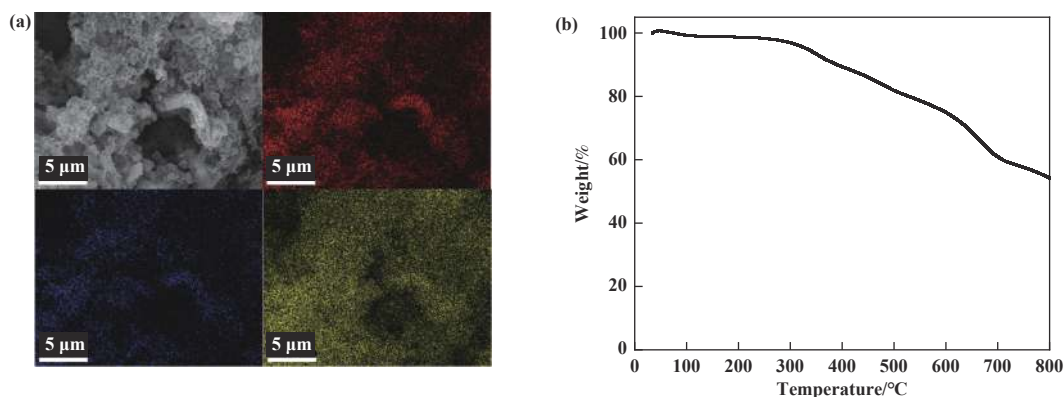


Fig.3 (a) SEM micrograph of the MT-CTF, and corresponding EDX mapping (Color code: C, red; N, blue; S, yellow; Scale: 5 μm); (b) Thermogravimetric analysis (TGA) of MT-CTF

Therefore, the fast kinetics can be attributed to the intrinsic promising properties of MT-CTF, such as porous structures and the chelating sites with Hg^{2+} .

The distribution coefficient (K_d) for Hg^{2+} removal by the present adsorbents was calculated as per the following equation (4)^[37], i.e. K_d :

$$K_d = \frac{C_0 - C_e}{C_e} \times \frac{V}{m} \quad (4)$$

The K_d value clearly shows the affinity of a adsorbent for metal ions^[24]. The calculated K_d is estimated to be 5.4×10^7 . The obtained high K_d value suggests that MT-CTF has great potential for Hg^{2+} adsorption. As reported, K_d value can be significantly affected by intrinsic properties of adsorbents, such as accessibility and affinity of the binding sites and flexibility

of functional groups^[38].

The pH value of the Hg^{2+} solution observably impacts the adsorption capacity. We then examined this over a wide pH range (from 1 to 12). As depicted in Fig. 4(d), the highest adsorption efficiency of MT-CTF was achieved to be 99.7% at the pH of 7^[39]. The maximum adsorption of Hg^{2+} on MT-CTF was estimated to be $751 \text{ mg} \cdot \text{g}^{-1}$, ranking at the top among previously-reported adsorbents(Fig.5(a)), while the CTF-1 has no effect on Hg. Furthermore, stable separation performance was clearly observed, suggesting exceptional binding affinity of MT-CTF towards Hg^{2+} . In addition, the selectivity plays a crucial role in achieving high separation performance. Towards this end, a wide variety of metal ions were examined for the

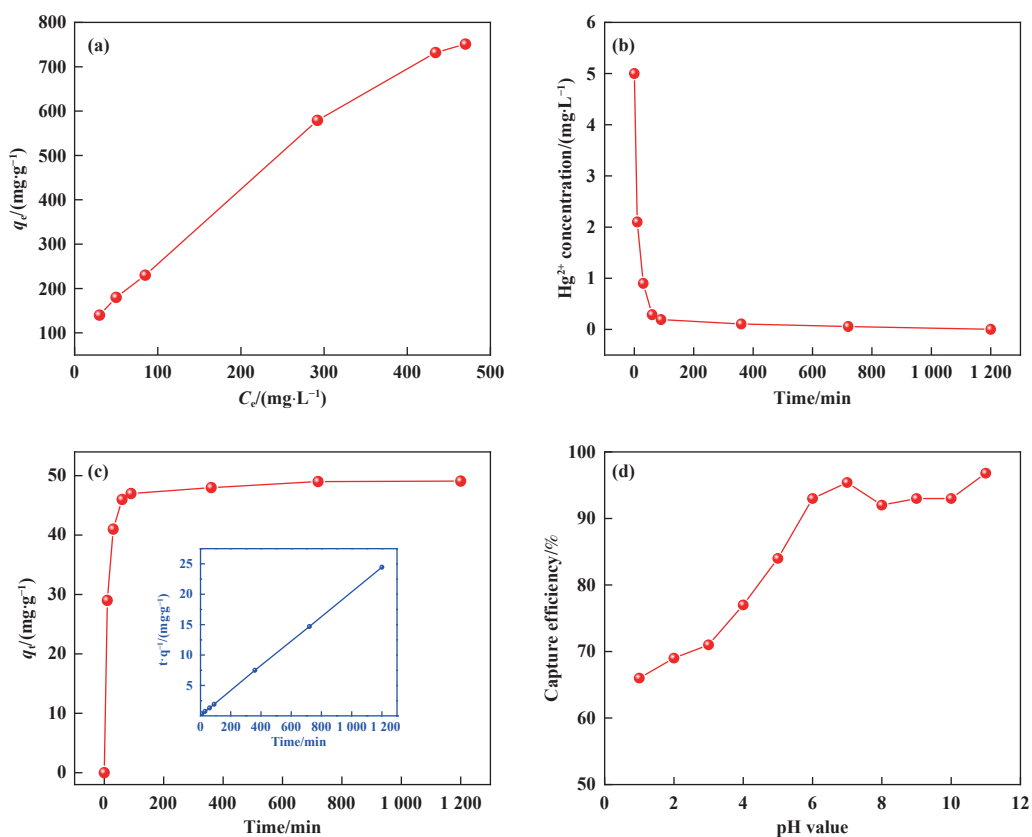


Fig.4 (a) Hg²⁺ adsorption isotherm for MT-CTF; (b) Hg²⁺ sorption kinetics of MT-CTF with Hg²⁺ initial concentration of 5 mg·L⁻¹; (c) Adsorption curve of Hg²⁺ versus contact time in aqueous solution using MT-CTF. Inset shows the pseudo-second order kinetic plot for the adsorption; (d) Adsorption performance under different pH

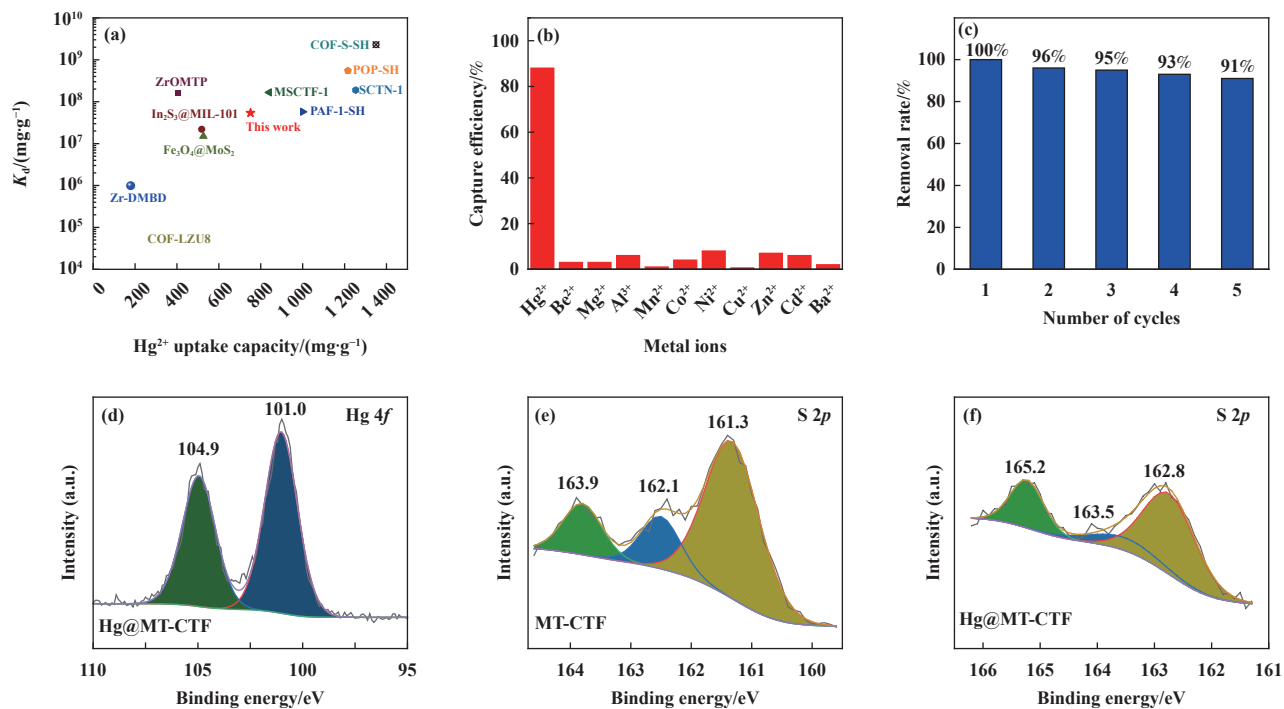


Fig.5 (a) Comparison of Hg²⁺ saturation uptake amount and K_d value for MT-CTF with other porous materials; (b) Adsorption selectivity for Hg²⁺ of MT-CTF in mixed metal solution; (c) Recycling performance of MT-CTF; XPS spectra for (d) Hg 4f of Hg@MT-CTF, (e) S 2p of MT-CTF, and (f) S 2p of Hg@MT-CTF

adsorption using MT-CTF as the adsorbent. The initial batches were carried out using the solution containing Hg^{2+} , Be^{2+} , Mg^{2+} , Al^{3+} , Mn^{2+} , Co^{2+} , Ni^{2+} , Cu^{2+} , Zn^{2+} , Cd^{2+} and Ba^{2+} . As shown in Fig. 5(b), MT-CTF exhibits an excellent selectivity of Hg^{2+} , which originates from the existence of rich task-specific methylthio groups. Given the fact that the reusability of adsorbents is a key parameter governing their separation applications, we further examined the recyclability of MT-CTF. As shown in Fig. 5(c), excellent cycling performance was obtained, where no significant adsorption loss was observed after five consecutive cycles, suggesting intrinsic robust structure of MT-CTF. As shown in the XPS spectra, two signals at 101.0 and 104.9 eV, corresponding to $\text{Hg} 4f_{7/2}$ and $4f_{5/2}$ respectively provide strong evidence of successful capture of Hg^{2+} within the pores of MT-CTF. The methylthio sites inside MT-CTF were confirmed by the peaks at 161.3 eV ($S 2p_{3/2}$) and 162.1 eV ($S 2p_{1/2}$), whereas these two peaks were shifted to 162.8 eV ($S 2p_{3/2}$) and 163.5 eV ($S 2p_{1/2}$) due to the interaction with Hg^{2+} ($\text{Hg}@\text{MT-CTF}$, Fig. 5(e) and Fig. 5(f)).

3 Conclusion

In summary, a crystalline CTF with methylthio pendant arms was rationally synthesized for efficient Hg^{2+} adsorption. MT-CTF was prepared through a low-temperature-involved condensation reaction between methylthio-functionalized aromatic aldehydes and amidine moieties. Due to the existence of rich task-specific methylthio groups, MT-CTF exhibits an exceptional Hg^{2+} uptake capacity of $751 \text{ mg}\cdot\text{g}^{-1}$, accompanied with high selectivity over a wide range of metal ions, where exceptional removal efficiency over a wide pH range with excellent recyclability was also achieved. In the future, we will investigate the adsorption performance of MT-CTF in domestic and industrial wastewater, and evaluate the long-term stability and practicability of the MT-CTF. We anticipated that this work may open up new possibility in the synthesis of CTFs for promising separation applications.

References

- Jyethi D S. Air quality: Global and regional emissions of particulate matter, SO_x and NO_x [M]. *Plant Responses to Air Pollution*, Kulshrestha U, Saxena P, Eds. Springer Singapore: Singapore, 2016: 5–19.
- Oberschelp C, Pfister S, Raptis C E, et al. Global emission hotspots of coal power generation[J]. *Nat Sustain*, 2019, **2**(2): 113–121.
- Lv S W, Liu J M, Wang Z H, et al. Recent advances on porous organic frameworks for the adsorptive removal of hazardous materials[J]. *J Environ Sci*, 2019, **80**: 169–185.
- Zahir F, Rizwi S J, Haq S K, et al. Low dose mercury toxicity and human health, environmental toxicology and pharmacology[J]. *Environ Toxicol Pharmacol*, 2005, **20**(2): 351–360.
- Liu J, Zhang X H, Tran H, et al. Heavy metal contamination and risk assessment in water, paddy soil and rice around an electroplating plant[J]. *Environ Sci Pollut Res*, 2011, **18**(9): 1623–1632.
- Yu J G, Yue B Y, Wu X W, et al. Removal of mercury by adsorption: A review[J]. *Environ Sci Pollut Res*, 2016, **23**(6): 5056–5076.
- Zhou Q Q, Yang N, Li Y Z, et al. Total concentrations and sources of heavy metal pollution in global river and lake water bodies from 1972 to 2017[J]. *Glob Ecol Conserv*, 2020, **22**: e00925.
- Zhang Y, Li Q, Sun L, et al. High efficient removal of mercury from aqueous solution by polyaniline/humic acid nanocomposite[J]. *J Hazard Mater*, 2010, **175**(1): 404–409.
- Duan X L, Yuan C G, Jing T T, et al. Removal of elemental mercury using large surface area micro-porous corn cob activated carbon by zinc chloride activation[J]. *Fuel*, 2019, **239**: 830–840.
- Kong Y, Wang L, Ge Y Y, et al. Lignin xanthate resin-bentonite clay composite as a highly effective and low-cost adsorbent for the removal of doxycycline hydrochloride antibiotic and mercury ions in water[J]. *J Hazard Mater*, 2019, **368**: 33–41.
- Li Y, Yang L Y, Li X X, et al. A composite adsorbent of ZnS nanoclusters grown in zeolite NaA synthesized from fly ash with a high mercury ion removal efficiency in solution[J]. *J Hazard Mater*, 2021, **411**: 125044.
- Huang N, Zhai L P, Xu H, et al. Stable covalent organic frameworks for exceptional mercury removal from aqueous solutions[J]. *J Am Chem Soc*, 2017, **139**(6): 2428–2434.
- Zabih M, Asl A H, Ahmadpour A. Studies on adsorption of mercury from aqueous solution on activated carbons prepared from walnut shell[J]. *J Hazard Mater*, 2010, **174**(1): 251–256.
- Sarafraz H, Minuchehr A, Alahyarizadeh G, et al. Synthesis of enhanced phosphonic functional groups mesoporous silica for uranium selective adsorption from aqueous solutions[J]. *Sci Rep*, 2017, **7**(1): 11675.
- Zheng J J, Zhang X W, Zhang Y, et al. Structural effects of hierarchical pores in zeolite composite[J]. *Micropor Mesopor Mat*, 2009, **122**(1/3): 264–269.
- Ren X Y, Shi Y Z, Zheng H, et al. A novel covalent organic polymer with hierarchical pore structure for rapid and selective trace $\text{Hg}(\text{II})$ removal from drinking water[J]. *Sep Purif Technol*, 2022, **285**: 120306.
- Wang N, Ouyang X K, Yang L Y, et al. Fabrication of a magnetic cellulose nanocrystal/metal-organic framework composite for removal of $\text{Pb}(\text{II})$ from water[J]. *ACS Sustain Chem Eng*, 2017, **5**(11): 10447–10458.
- Gatou M A, Bika P, Stergiopoulos T, et al. Recent advances in covalent organic frameworks for heavy metal removal applications[J]. *Energies*, 2021, **14**(11): 3197.
- a. Krishnaraj C, Jena H S, Leus K, et al. Covalent triazine frameworks—a sustainable perspective[J]. *Green Chem*, 2020, **22**(4): 1038–1071.
b. Zhang Z Y, Shi C C, Zhang X, et al. Carbazole-based covalent organic frameworks for photocatalytic hydrogen evolution [J]. *J Mol Catal (China)*, 2023, **37**(4): 367–374.
c. Zhang Z Y, Zhang X, Shi C C. Covalent organic frameworks supported noble-metal Pt for electrocatalytic hydrogen evolution[J]. *J Mol Catal (China)*, 2024, **38**(1): 42–50.
d. Li B Y, He F G, Zhang M H, et al. Modification of metal organic framework materials and their application in photo-catalytic hydrogen evolution[J]. *J Mol Catal (China)*, 2023, **37**(1): 94–107.
- Zhu X, Tian C C, Mahurin S M, et al. A superacid-catalyzed synthesis of porous membranes based on triazine frameworks for CO_2 separation[J]. *J Am Chem Soc*, 2012, **134**(25): 10478–10484.
- Ji Y, Ni C L, Jiang Z H, et al. Removal of mercury ions from water by triazine porous organic polymers rich in nitrogen and oxygen groups[J]. *J Mol Struct*, 2024, **1298**: 137066.
- Leus K, Folens K, Nicomel N R, et al. Removal of arsenic and mercury species from water by covalent triazine framework encapsulated $\gamma\text{-Fe}_2\text{O}_3$ nanoparticles[J]. *J Hazard Mater*, 2018, **353**: 312–319.
- Ding S Y, Dong M, Wang Y W, et al. Thioether-based fluorescent covalent organic framework for selective detection and facile removal of mercury(II)[J]. *J Am Chem Soc*, 2016, **138**(9): 3031–3037.
- Rajalakshmi K, Muthusamy S, Xie M, et al. Fabrication of thio-phenene decorated side chain entanglement free COFs for highly regenerable mercury extraction[J]. *Chem Eng J*, 2022, **430**: 1331449.
- Khojastehnezhad A, Moeinpour F, Jafari M, et al. Postsynthetic modification of core-shell magnetic covalent organic frameworks for the selective removal of mercury[J]. *ACS Appl Mater Interfaces*, 2023, **15**(23): 28476–28490.
- Xiong C J, Wang H, Zhang Z B, et al. Triazine-based sulphur-containing polymers for Hg^{2+} adsorption: Efficiency and mechanism[J]. *Polymer*, 2023, **289**: 126480.
- Yang Z L, Gu Y Y, Yuan B L, et al. Thio-groups decorated covalent triazine frameworks for selective mercury removal[J]. *J Hazard*

- Mater*, 2021, **403**: 123702.
- [28] Wang K W, Yang L M, Wang X, *et al.* Covalent triazine frameworks via a low - temperature polycondensation approach[J]. *Angew Chem Int Ed*, 2017, **56**(45): 14149–14153.
- [29] Yamamoto T, Nishimura T, Mori T, *et al.* Largely π -extended thienoacenes with internal thieno[3,2-b]thiophene substructures: Synthesis, characterization and organic field-effect transistor applications[J]. *Org Lett*, 2012, **14**(18): 4914–4917.
- [30] Yang N, Gu Y Q, Shan Y L, *et al.* Dual rate-modulation approach for the preparation of crystalline covalent triazine frameworks displaying efficient sodium storage[J]. *ACS Macro Lett*, 2021, **11**(1): 60–65.
- [31] Wang H, Jiang D N, Huang D L, *et al.* Covalent triazine frameworks for carbon dioxide capture[J]. *J Mater Chem A*, 2019, **7**(40): 22848–22870.
- [32] Wang W J, Liu J, Yan Y T, *et al.* Uncommon thioether-modified metal-organic frameworks with unique selective CO₂ sorption and efficient catalytic conversion[J]. *CrystEngComm*, 2021, **23**(6): 1447–1454.
- [33] Liu M Y, Jiang K, Ding X, *et al.* Controlling monomer feeding rate to achieve highly crystalline covalent triazine frameworks[J]. *Adv Mater*, 2019, **31**(19): 1807865.
- [34] Zhang S Q, Cheng G, Guo L P, *et al.* Strong - base - assisted synthesis of a crystalline covalent triazine framework with high hydrophilicity via benzylamine monomer for photocatalytic water splitting[J]. *Angew Chem Int Ed*, 2020, **132**(15): 6063–6070.
- [35] Jia Y, Zhu D H, Yang Q F, *et al.* Triazole and methylthio modified covalent organic frameworks for enhancing Hg(II) adsorption from water[J]. *Mater Today Commun*, 2024, **38**: 107976.
- [36] Anbazhagan R, Krishnamoorthi R, Kumaresan S, *et al.* Thioether-terminated triazole-bridged covalent organic framework for dual-sensitive drug delivery application[J]. *Mater Sci Eng C*, 2021, **120**: 111704.
- [37] Sun Y K, Ding Y Q, Zhou W W, *et al.* Synthesis and selective Au(III) adsorption of ureido polymers containing large repeating rings[J]. *ACS Omega*, 2021, **6**(42): 28004–28011.
- [38] Chen L Y, Tang J L, Zhang X Y, *et al.* A novel benzothiazole modified chitosan with excellent adsorption capacity for Au(III) in aqueous solutions[J]. *Int J Biol Macromol*, 2021, **193**: 1918–1926.
- [39] Fan C Y, Wu H, Guan J Y, *et al.* Scalable fabrication of crystalline cof membranes from amorphous polymeric membranes[J]. *Angew Chem Int Ed*, 2021, **60**(33): 18051–18058.

用于高效吸附汞 (II) 的含有甲基硫侧链的共价三嗪框架

娄艺晓^{1,2}, 周路路³, 杨娜¹, 朱祥^{1*}

(1. 中国科学院兰州化学物理研究所 羰基合成与选择氧化国家重点实验室, 甘肃 兰州 730000;

2. 中国科学院大学, 北京 100049; 3. 华东理工大学 资源与环境工程学院, 上海 200237)

摘要: 通过物理分离过程可缓解环境污染问题, 这一策略激发了人们对具有优异吸附能力的新型纳米多孔材料的研究兴趣. 共价三嗪框架 (CTFs) 作为共价有机框架 (COFs) 材料的一种, 具有大孔隙度、高稳定性和丰富的氮原子掺杂等特性, 在吸附分离中被广泛研究和应用. 开发用于高效吸附汞 (II) (Hg²⁺) 的 CTFs 材料在该领域具有重要的意义, 但是由于合成策略有限以及基于离子热法衍生的传统 CTFs 的结构-性能之间的关系尚不明确, 因此很少尝试. 我们设计合成了 1 种含有甲基硫侧链的结晶性 CTFs 用于高效去除 Hg²⁺, 吸附容量为 751 mg·g⁻¹, 与先前报道的 Hg²⁺ 吸附剂相比, 性能优异, 这项工作可能为实现多种分离应用的 COFs 的合成提供更多可能性.

关键词: 共价三嗪框架; 甲基硫侧链; 汞吸附; 结构-性能关系